2022

Computational Model Of Start-up Process for Reciprocating Compressors

Eduardo Postingel Falcetti

Tiago Fernando Botega

Luben Cabezas Gomez

Computational Model of Start-up Process for Reciprocating Compressors

Eduardo P. FALCETTI[1,2*], Tiago F. BOTEGA[1], Luben CABEZAS-GÓMEZ[2]

[1] Tecumseh Products Company,
São Carlos, São Paulo, Brazil
eduardo.falcetti@tecumseh.com

[2] Heat Transfer Research Group, Department of Mechanical Engineering, São Carlos School of Engineering, University of São Paulo
São Carlos, São Paulo, Brazil
lubencg@sc.usp.br

* Corresponding Author

ABSTRACT

The development of more efficient and optimized compressors depends on understanding the loads present during their start-up and steady operation in the refrigeration system. The loads arise mainly from the gas compression process in the cylinder, the pressure drop in the suction and discharge systems and the friction in bearings. During compressor start-up, the electric motor must supply the required torque to the mechanical kit to overcome these loads and accelerate the mechanism. Thus, the compressor start-up is considered critical in the design of compressors and its components, such as electric motors. This work aims to present the development of a computational model for simulating a reciprocating compressor start-up, considering the coupling between the induction electric motor and the mechanical system. The mechanical loads (friction from bearings and from fluid compression and pressure drop) are calculated coupled with the torque from the motor, considering the inertial forces in the mechanism. A 0D/1D fluid dynamic model was used to determine the flow in the compressor suction and discharge circuits, as well as in the cylinder compression process. A simplified motor model was used to represent the torque available in the motor as a function of the instantaneous angular velocity of the shaft/rotor. An experimental start-up study using an instrumented compressor determined the movement of the mechanical kit, as well as the pressure variation in the system through pressure transducers and encoder installed in established regions. The experimental results presented are used to validate the numerical model and demonstrate its capacity to simulate the compressor starting operation with a satisfactory accuracy. Finally, a parametric analysis indicated the main components that impact the starting process.

1. INTRODUCTION

The design of new compressors deals with market competitiveness challenges, mainly in the search for cost reduction and increasingly aggressive efficiency requirements. The compressor commonly applied in light commercial and household applications is the reciprocating compressor that employs a reciprocating mechanism to compress the fluid. In addition, the electric motor used in these compressors is generally a single-phase induction motor.

In the search for loss reduction in these compressors, aiming an increasing efficiency, a component that stands out is the electric motor. It is responsible for providing the required torque to the mechanism. It can be represented by an electrical efficiency, when combined with the starting and operating electrical components, such as capacitors. Possamai and Todescat (2004) indicated that this efficiency can reach 87.3% for a compressor operating at R134a and 60Hz. The results from Dutra and Deschamps (2015) show that this efficiency can vary substantially depending on the operating condition, that affects the required torque.

In this way, knowing the operating condition of a compressor and the required torque is fundamental in the design of electric motors. In this context, the operating conditions can be divided according to the characteristic of the phenomenon into steady state and transients conditions.

The steady state conditions are characterized by a stable operation, i.e., the mechanical, thermodynamic and electrical

properties do not have a significant variations over time. For this type of condition, some works are presented, such as (Li, 2012; Negrão, Erthal, Andrade, & Da Silva, 2011) that use experimental data to characterize the compressors. These semi-empirical models have a good ability to predict performance data, but generally require a considerable number of experimental performance tests.

Other models consider 1D/0D approaches to represent the flow and movement of the mechanism (Ussyk, 1984; Fagotti, Todescat, Ferreira, & Prata, 1994; Dutra & Deschamps, 2015). These models present a very good prediction of performance. Dutra and Deschamps (2015) stands out for the incorporation of a simplified electric motor model, which included the ability to predict torque and electrical losses. This model allows a good thermal diagnosis of the compressor and understanding of the loss segregation in steady-state applications. On the other hand, Dutra and Deschamps (2015) represented the motor as an equivalent circuit and this simplification does not allow its use in conditions with fast transients (Chen, 2004).

Conditions that represent fast transients in the compressor are generally encountered under start and stop operational phases of the compressor. Some simplified models seek to represent this phenomenon as in Fagotti et al. (1994); Kim (2004); Porkhial, Khastoo, and Modarres Razavi (2002). The model presented by Link and Deschamps (2011) employs a similar approach to Ussyk (1984) for the hydrodynamic and mechanical model. Link and Deschamps (2011) applied the motor torque-speed curve measured to represent the electric motor.

In general, the friction models in bearings found in the works employ simplifications, as in Link and Deschamps (2011), who considers the Stribeck curve model. This model required adjustment of transition rotation of lubrication regime calibrated through experimental data of instantaneous rotation of the compressor.

Therefore, this work seeks to develop a reciprocating compressor model using a single-phase induction motor capable of representing the transient phenomena encountered during compressor start-up. The hydrodynamic model represents a 0D/1D model and a 2D model for the mechanism. On the other hand, the bearing model employs the mobility method coupled with the contact model from Greenwood and Williamson (1966). Thus, it is expected to represent the lubrication transition directly without the need for previous instrumented compressor tests for adjustments.

2. METHODOLOGY

In this section will be presented the details of the computational model and experimental test applied. The experimental tests were performed with an instrumented compressor to determine the transient pressures in the inlet and outlet of the compressor during the start-up process. Furthermore, the compressor speed was measured. The obtained experimental data were compared with simulated numerical results obtained with the computational model.

The computational model presented in this article is that solved in the GT-Power software from Gamma Technologies, LLC. The compressor model is divided into two distinct models for convenience, the mechanical and the hydrodynamic. The mechanical model determines the movement of the reciprocating mechanism based on mechanical joints and external loads, including gas loads, motor torque and bearing friction. The hydrodynamic model evaluates the fluid flow through the suction circuit, discharge circuit, valves and compressor cylinder. In the next sections, details about each model will be described, as well as the applied boundary and initial conditions.

2.1 Mechanical Model

The reciprocating mechanism has different components, such as connecting rod, shaft, crankcase, piston and rotor (motor), as presented in figure 1. In the mechanical model described in this work all bodies are considered rigid. By this reason the mechanical formulation considers a 2D rigid multi-body system. The crankcase is considered fixed in the inertial reference frame.

The bodies movement is described by the Newton-Euler system of equations, presented in equation 1. However, following the augmented formulation in state space format, presented by Shabana (2010), the position vector can be determined according to the equation 2. The matrix $\boldsymbol{M}$ represents the mass matrix of the system, while the vector $\ddot{\boldsymbol{q}}$ represents the linear and angular accelerations of the bodies. The vectors $\boldsymbol{Q_e}$ and $\boldsymbol{Q_c}$ are the external forces and constraints of the system, respectively. The mass matrix $\overline{\boldsymbol{M}}_i^{-1}$ is associated with the independent coordinates and the vector $\overline{\boldsymbol{Q}}_i$ is the generalized forces associated with the independent coordinates.

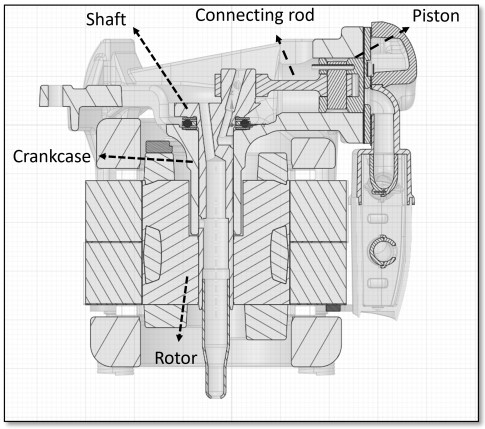

Figure 1: Schematic representation of compressor geometry

The initial condition of the mechanical system considers all bodies at rest, that is, zero initial velocity. The starting position of the mechanism is considered at the bottom dead center (crank angle of 180°).

$$\boldsymbol{M}\ddot{\boldsymbol{q}} = \boldsymbol{Q}_e + \boldsymbol{Q}_c \tag{1}$$

$$\dot{\boldsymbol{y}} = \begin{bmatrix} \dot{\boldsymbol{y}}_1 \\ \dot{\boldsymbol{y}}_2 \end{bmatrix} = \begin{bmatrix} \dot{\boldsymbol{y}}_1 \\ \dot{\boldsymbol{G}}_i(y,t) \end{bmatrix} \tag{2}$$

$$\ddot{\boldsymbol{q}}_i = \overline{\boldsymbol{M}}_i^{-1}\overline{\boldsymbol{Q}}_i = \boldsymbol{G}_i(\boldsymbol{q}_i, \dot{\boldsymbol{q}}_i, t) \tag{3}$$

The connection between the bodies is defined as mechanical joints according to table 1. For revolution joints, bearing formulations are considered to determine external torques due to friction. The method applied to represents the bearings is the mobility, as shown by J. F. Booker (1971). The mobility model is widely used for reciprocating mechanisms and makes it possible to determine the position of the bearings through the forces applied to the joint reaction and relative instantaneous velocity (J. Booker, 2014). This formulation employs maps that were obtained by solving Newton's equations as presented in J. F. Booker (1965) and J. F. Booker (1969).

Table 1: Rigid bodies and joints connection between them

Body/Body	**Connecting rod**	**Crankcase**
Crankshaft	Revolute joint	Revolute joint
Piston	Revolute joint	Prismatic joint

To determine the transition of lubrication regimes, the mobility model is coupled with the contact model of Greenwood and Williamson (1966). Therefore, the total reaction force at the joint F is a composition of the contact force F_c and the hydrodynamic force F_h from the oil film according to equation 4. The properties of the surface roughness are determined as the method presented by Tomanik, Chacon, and Teixeira (2003). The oil properties consider the mixture between oil and refrigerant fluid as discussed in Seeton and Hrnjak (2006). Therefore, the equivalent density $\rho = \rho(p,T)$ and equivalent viscosity $\mu = \mu(p,T)$ depends on the pressure and temperature of the mixture.

$$\boldsymbol{F}_h = \boldsymbol{F} - \boldsymbol{F}_c \tag{4}$$

The friction force between piston and cylinder is determined according to equation 5, where the friction coefficient or damping proportional to velocity c_p is determined considering a Couette flow. Another external load present in the mechanical system comes from the compression of the gas in the cylinder. It is determined through equation 7 that represents the force balance between the force from the housing pressured p_{in} and the cylinder pressure p_{cyl}.

$$F_p = c_p U_p \tag{5}$$

$$c_p = \frac{\mu \pi D_p L_p}{\delta_p} \tag{6}$$

$$F_p = \oint_S p \times dA = \frac{\left(p_{cyl} - p_{in}\right) \pi D_{cyl}^2}{4} \tag{7}$$

The torque from the motor was adjusted according the equation 8 proposed by Bukac (2002) from dynamometer motor tests, performed previously. The motor slip s is determined by the equation 9 considering the motor synchronous speed ω_s. The coefficients B1, B2 and B3 were determined for two different electric motor temperatures (25°C and 120°C), as shown in figure 2. The speed ratio is the relation between speed and syncronous motor speed $\omega^* = \frac{\omega}{\omega_s}$. For intermediate temperatures, linear interpolations between the curves are applied to estimate the motor torque for each motor speed. Through the determined coefficients, the torques for other motor voltages can be determined simply by correcting the motor voltage (V_m) in the equation 8.

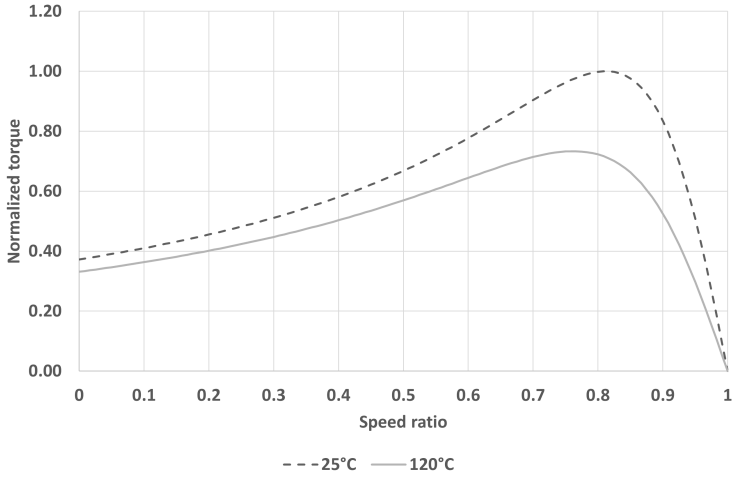

Figure 2: Motor torque curves for two different motor temperatures

$$T_m = V_m^2 \frac{B_1 s}{B_2 s^2 + B_3 s + 1} \tag{8}$$

$$s = \frac{\omega_s - \omega}{\omega_s} \tag{9}$$

The movement of the suction and discharge valves are determined considering a 1D damped mass-spring system, according to equation 10. This approach is applied widely in different works (Dutra & Deschamps, 2015; Bell et al.,

2020; Link & Deschamps, 2011). The external force from the gas F is determined through the effective force area. This coefficient was determined previously through 3D CFD analysis of the valve for different valve lifts. A similar approach to the work presented by Ferreira and Gasche (2019). The equivalent mass m_{eq}, the stiffness k, and damping factor c was determined from a 3D static structural analysis and 3D modal analysis of the valves as discussed in Gasche, Dias, Bueno, and Lacerda (2016).

$$m_{eq}\ddot{x} = -kx - c\dot{x} + F(t) \tag{10}$$

2.2 Flow Model

The hydrodynamic model employs 0D/1D discretization to represent the suction circuit, discharge circuit and cylinder. This model applies a staggered grid that represents the vector quantities at the boundaries of the control volume and scalar quantities at the center of the control volume. The conservation of mass equation 11, the conservation of energy equation 12 and the conservation of momentum equation 13 are solved in the explicit format. The flow system is assumed adiabatic because the transient phenomena presented in the start-up process are very fast.

The compressor presented in this work uses the fluid refrigerant propane (R290). The fluid properties are obtained from the reference fluid thermodynamic and transport properties database REFPROP (Lemmon, Bell, Huber, & McLinden, 2018).

$$\frac{dm}{dt} = \sum_{boundaries} \dot{m} \tag{11}$$

$$\frac{d(me)}{dt} = -p\frac{dV}{dt} + \sum_{boundaries} \dot{m}H \tag{12}$$

$$\frac{d\dot{m}}{dt} = \frac{1}{dx}\left(dpA + \sum_{face} \dot{m}u - S_f - S_k\right) \tag{13}$$

The pressure drop due to the friction in tubes is considered in the source term S_f, which considers the fanning friction factor f. The S_k source term determines the pressure drop from bends, tapers and restrictions. The coefficient K is determined from Miller (1999) for the different geometries.

$$S_f = 4f\frac{\rho u|u|}{2}\frac{dx}{D} \tag{14}$$

$$S_k = \frac{1}{2}K\rho u|u| \tag{15}$$

The mass flow rates through the suction and discharge valves is determined applying the discharge coefficients C_d, which were determined previously from CFD 3D analysis for different valve lifts as discussed in Ferreira and Gasche (2019). The leakage between the cylinder and piston is determined considering the Coette flow, calculated from the equation 16.

$$\dot{m} = \pi D\delta\left(\frac{\delta^2\Delta p}{12\mu L} - \frac{1}{2}U_{piston}\right) \tag{16}$$

The compressor inlet and outlet pressures are defined as a transient signal. The pressures were previously obtained from measurements in an instrumented compressor during the start-up test. The inlet temperature is considered constant, also previously obtained by measurements. The initial pressure of the system is considered the same as the pressure equalized between suction and discharge sections. The initial internal temperature was considered the same measured at the compressor inlet. In the compressor outlet was considered the Newman's boundary condition for temperature, therefore the temperature gradient was defined null ($\nabla T = 0$).

2.3 Experimental Test

In the start-up test, the compressor suction and discharge initial pressures are equalized. As soon as the compressor starts to rotate, there is an imbalance between suction and discharge pressures. This phenomenon occurs because the compressor removes mass from the volume connected to suction and pumps it to the volume connected to discharge. The electrical voltage applied to the motor is controlled during the test. A calorimeter equipment was used to perform the start-up test.

The measurement points of the instrumented compressor are presented in figure 3. As discussed previously, the measured values of pressure at the compressor suction and discharge tubes and of temperature at the compressor inlet and in the motor stator are used as input parameters in the computational model.

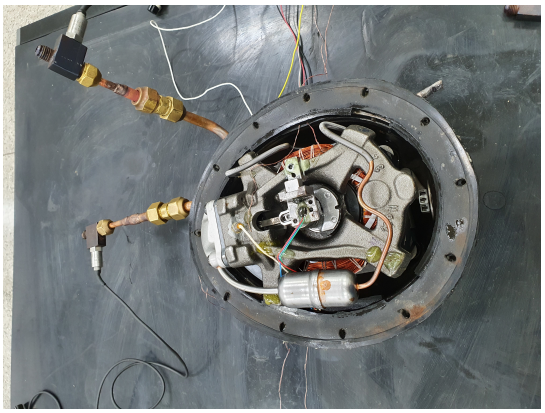

Figure 3: Instrumented compressor applied in start-up test

The suction and discharge pressures are measured using pressure transducers. The instantaneous position (crank angle) of the mechanism is obtained using a rotary encoder. Temperature measurements are performed by thermocouples. The errors attributed to each instrument measurement are presented in table 2.

Table 2: Measurement errors determined from instrumentation specification

Suction pressure	±0.25%
Discharge pressure	±0.25%
Angular position	±1%
Inlet temperature	±1°C
Motor temperature	±1°C

3. RESULTS

This section is divided into two different parts. In the first, it is performed a comparison between the numerical and experimental results. This comparison is used for validating the computational model. In the second part, a parametric analysis is addressed for the main variables that characterize the motor operation.

The computational results of the compressor speed for the motor tension of 198V are compared with the experimental results during the start-up process, as presented in figure 5. The compressor speed presented in figure 5 is a moving average from the instantaneous speed. The speed results are presented in the speed ratio format that is determined by the relation between the speed and synchronous motor speed $\omega^* = \frac{\omega}{\omega_s}$.

The transient pressures at the compressor inlet and outlet were measured as shown in figure 4. The pressures are expressed in the normalized format by the equalized pressure $p^* = \frac{p}{p_{eq}}$. The motor temperature was measured during the test and the average temperature obtained was $75°C$. The inlet temperature measured at the initial instant of the start-up process was $35°C$.

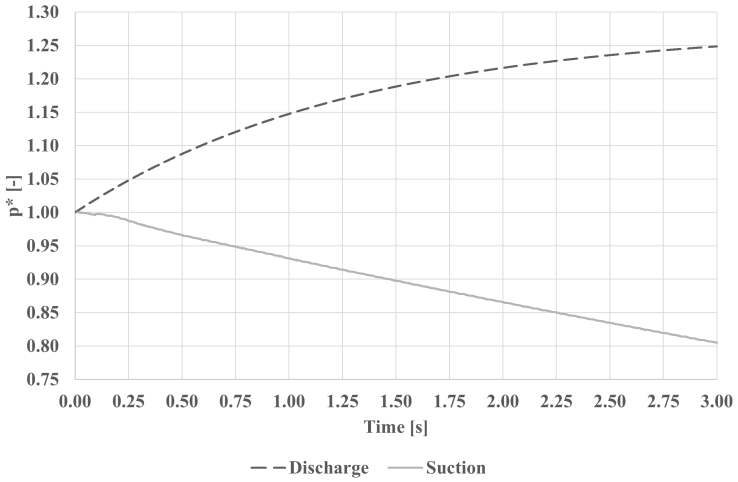

Figure 4: Suction and discharge pressures measured in compressor start-up test

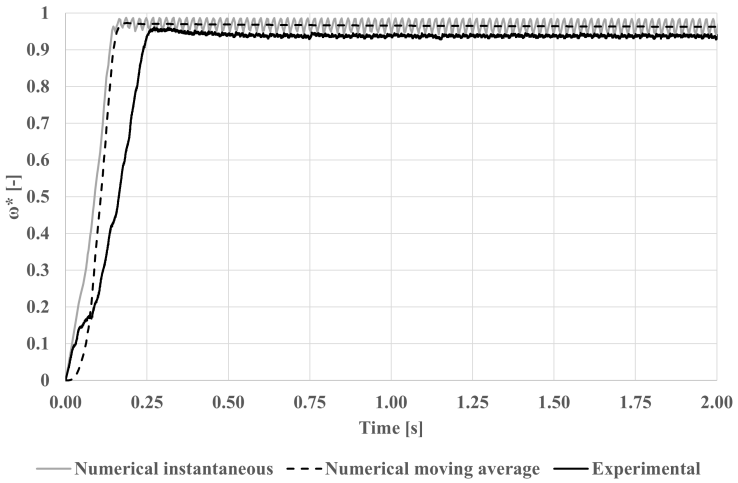

Figure 5: Compressor speed comparison between experimental and numerical results in start-up test

The compressor speed from the computational model has a tendency to reach the stable condition sooner than the experimental results. However, the difference between the moving average from the numerical model and the experimental data after the stable operational condition is around 2.2%. From angular position presented in figure 6 is possible to notice the very similar behavior of the numerical and experimental results for the stable operational state ($t = 0.25s$).

The higher acceleration in the numerical results can be explained by underestimation of the load torque from the mechanism. The bearings models are considered without an eccentricity between the bearing and journal at the initial instant of the simulation. Therefore, the friction torque can be underestimated.

A parametric analysis for the motor tension and temperature were performed with the same transient pressure signals presented in figure 4. The compressor speed results for different motor temperatures are presented in figure 7(a). The increasing in motor temperature decreases the motor torque available, as observed in figure 2. Therefore, the

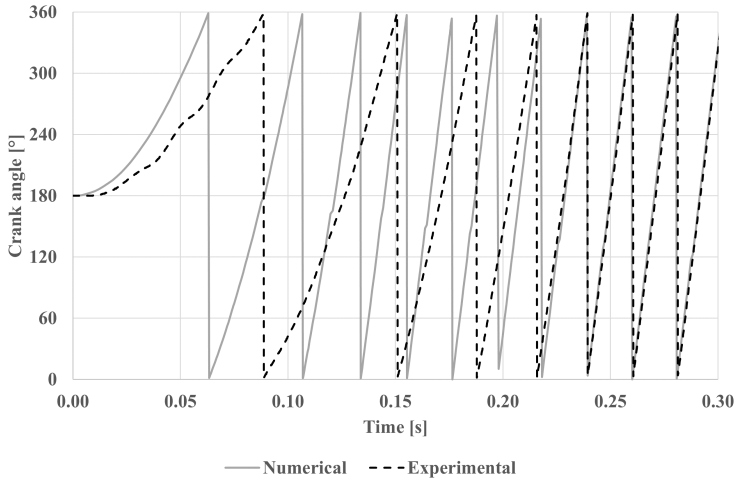

Figure 6: Comparison between numerical and experimental results of shaft angular position in compressor start-up

compressor with the lower motor temperature tends to reach the stable condition sooner than with the higher motor temperatures.

The motor tension influence on compressor speed is presented in figure 7(b). From equation 8 is possible to conclude that the increment in motor tension increases the torque. This is the reason that the compressor model applied with highest motor tension reached the stable condition sooner than the other tensions. The motor tension had a higher impact in compressor speed than the motor temperature. This behavior is related to the quadratic term presented in equation 8.

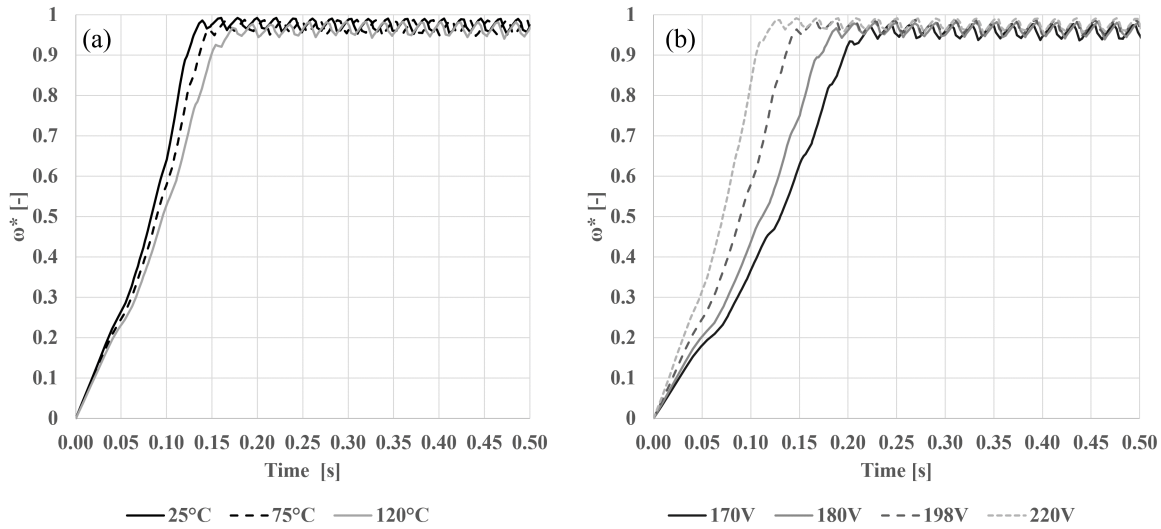

Figure 7: Comparison of numerical results of compressor instantaneous speed for different motor temperatures (a) and motor tensions (b) in compressor start-up

4. CONCLUSIONS

The experimental and numerical results of this work indicate that the computational model overestimated the compressor acceleration in the first moments of the start-up. This behavior can be related to the underestimation of the load torque during the initial moments. Otherwise, the model has very good agreement for the stable compressor operational conditions. This fact suggests that the model could be a possible tool for investigations of long-range temporal nature

during the compressor start-up, for example, the compressor stall. Furthermore, this work demonstrates the negative impact of motor temperature and positive impact of motor voltage on compressor acceleration during start-up. The investigation of different bearing models and initial conditions for the initial friction phenomena in the compressor start-up could improve the performance of the employed computational model. Furthermore, the boundary condition of suction and discharge pressures can be evaluated from simplified refrigeration system models, reducing strongly the dependency of experimental results of the model.

NOMENCLATURE

The nomenclature should be located at the end of the text using the following format:

A	area	(m^2)
B_1	motor torque constant	$(N\,m/V^2)$
B_2	motor torque constant	$(V^2/N/m)$
B_3	motor torque constant	$(V^2/N/m)$
c	damping coefficient	$(N\,s/m)$
C_d	discharge coefficient	$(-)$
D	diameter	(m)
e	internal energy	(J/kg)
$\boldsymbol{F}$	force	(N)
f	fanning friction	$(-)$
H	enthalpy	(J/kg)
K_p	pressure drop coefficient	$(-)$
k	valve stiffness	(N/m)
L	length	(m)
$\mathbf{M}$	mass matrix	(kg)
m	length	(kg)
p	pressure	(Pa)
$\mathbf{Q}$	force vector	(N)
$\boldsymbol{q}$	position vector	(m)
S_f	flow source term	(kg/s^2)
S_k	flow source term	(kg/s^2)
s	motor slip	$(-)$
T	torque	$(N\,m)$
t	time	(s)
U	piston Velocity	(m/s)
u	flow velocity	(m/s)
V	volume	(m^3)
V_m	motor voltage	(V)
x	position	(m)
$\dot{\boldsymbol{y}}$	velocity vector	(m/s)
δ	radial clearance	(m)
μ	dynamic viscosity	$(Pa\,s)$
ω	motor angular velocity	(Hz)
Subscript		
c	constraint	
cyl	cylinder	
e	external	
i	independent coordinates	
in	housing	
m	motor	

REFERENCES

Bell, I., Ziviani, D., Lemort, V., Bradshaw, C., Mathison, M., Horton, W., … Groll, E. (2020). Pdsim: A general

quasi-steady modeling approach for positive displacement compressors and expanders. *International Journal of Refrigeration*, *110*, 310–322.

Booker, J. (2014). Mobility/impedance methods: a guide for application. *Journal of Tribology*, *136*(2).

Booker, J. F. (1965, 09). Dynamically Loaded Journal Bearings: Mobility Method of Solution. *Journal of Basic Engineering*, *87*(3), 537-546.

Booker, J. F. (1969, 07). Dynamically Loaded Journal Bearings: Maximum Film Pressure. *Journal of Lubrication Technology*, *91*(3), 534-537.

Booker, J. F. (1971, 01). Dynamically-Loaded Journal Bearings: Numerical Application of the Mobility Method. *Journal of Lubrication Technology*, *93*(1), 168-174.

Bukac, H. (2002). Modeling compressor start up. *In Proceedings of the Compressor Conference at Purdue*.

Chen, W. K. (2004). *The electrical engineering handbook*. Elsevier.

Dutra, T., & Deschamps, C. (2015). A simulation approach for hermetic reciprocating compressors including electrical motor modeling. *International journal of refrigeration*, *59*, 168–181.

Fagotti, F., Todescat, M., Ferreira, R., & Prata, A. (1994). Heat transfer modeling in a reciprocating compressor. *In Proceedings of the Compressor Conference at Purdue*.

Ferreira, R., & Gasche, J. (2019). Effective force area and discharge coefficient for reed type valves: A comprehensive data set from a numerical study. *International Journal of Refrigeration*, *103*, 287–300.

Gasche, J. L., Dias, A. D. S. d. L., Bueno, D. D., & Lacerda, J. F. (2016). Numerical simulation of a suction valve: comparison between a 3d complete model and a 1d model. *In Proceedings of the Compressor Conference at Purdue*.

Greenwood, J., & Williamson, J. (1966). Contact of nominally flat surfaces. *Proceedings of the royal society of London. Series A. Mathematical and physical sciences*, *295*(1442), 300–319.

Kim, I. H. H. W. O. I., Y.Y. (2004). Dynamic analysis of multibody systems for reciprocating compressor of household refrigerator. *In Proceedings of the Compressor Conference at Purdue*.

Lemmon, E. W., Bell, I., Huber, M. L., & McLinden, M. O. (2018). *NIST Standard Reference Database 23: Reference Fluid Thermodynamic and Transport Properties-REFPROP, Version 10.0, National Institute of Standards and Technology.*

Li, W. (2012). Simplified steady-state modeling for hermetic compressors with focus on extrapolation. *International journal of refrigeration*, *35*(6), 1722–1733.

Link, R., & Deschamps, C. (2011). Numerical modeling of startup and shutdown transients in reciprocating compressors. *International Journal of Refrigeration*, *34*(6), 1398–1414.

Miller, D. (1999). *Internal flow systems, 2nd edition'*.

Negrão, C., Erthal, R., Andrade, D., & Da Silva, L. (2011). A semi-empirical model for the unsteady-state simulation of reciprocating compressors for household refrigeration applications. *Applied Thermal Engineering*, *31*(6-7), 1114–1124.

Porkhial, S., Khastoo, B., & Modarres Razavi, M. (2002). Transient characteristic of reciprocating compressors in household refrigerators. *Applied Thermal Engineering*, *22*(12), 1391-1402.

Possamai, F. C., & Todescat, M. L. (2004). A review of household compressor energy performance.

Seeton, C. J., & Hrnjak, P. (2006). Thermophysical properties of co2-lubricant mixtures and their affect on 2-phase flow in small channels (less than 1mm). *In Proceedings of the International Refrigeration and Air Conditioning Conference at Purdue*.

Shabana, A. A. (2010). *Computational dynamics*. John Wiley Sons, Ltd.

Tomanik, E., Chacon, H., & Teixeira, G. (2003). A simple numerical procedure to calculate the input data of greenwood-williamson model of asperity contact for actual engineering surfaces. In *Tribology series* (Vol. 41, pp. 205–215). Elsevier.

Ussyk, M. (1984). *Numerical simulation of the performance of hermetic reciprocating compressors* (Unpublished master's thesis). Department of Mechanical Engineering, Federal University of Santa Catarina, Brazil.

ACKNOWLEDGMENT

We would like to thank the Application and Development Laboratory of Tecumseh Products Company of Brazil for all support during the starting test presented in this article.